

A Model for the Hysteresis of Concrete to Describe the Cyclic Fatigue of Reinforced Concrete Structures During an Earthquake

Attinger, Richard^a, Kluegel, Jens-Uwe^a

^a*NPP Goesgen-Daeniken, Daeniken, Switzerland, rattinger@kkg.ch*

Keywords: Earthquake, damage, cyclic fatigue, hysteresis, reinforced concrete, simulation.

1 ABSTRACT

The damage measure of an earthquake is indicated by the intensity. A certain intensity can be due to earthquakes of different characteristics. Earthquakes of short duration with large acceleration amplitudes can have the same intensity as earthquakes of long duration with lower acceleration amplitudes. This behaviour is explained in this paper by cyclic fatigue of concrete for reinforced concrete structures.

A model for the hysteresis for concrete is introduced with a stiffness reduction built-in at re-loading if a predefined strength limit is exceeded. This strength limit is set to the transition from the stable crack growth to the unstable crack growth and coincides with the fatigue strength.

In a first step, the hysteresis model for concrete is checked on the basis of a micromechanical model, where a section through a reinforced concrete wall is simulated by concrete elements with the hysteresis model included and of steel elements. In a second step, the hysteresis model for concrete is implemented into a finite element code where the consequences of earthquakes of different magnitudes to a reinforced concrete building are demonstrated.

Both implementations of the hysteresis model for concrete show the need of a increased acceleration amplitude to get the same damage when the duration of an earthquake is shortened, i.e. when the magnitude is lowered. One concludes from this statement that the peak ground acceleration (PGA) can not be the measure for the damage state of buildings.

2 INTRODUCTION

2.1 Damage potential of an earthquake to structures

Parameters related solely to the amplitude of the ground motion, such as the peak ground acceleration (PGA), are often poor indicators of structural damage. For example, a large recorded PGA associated with a short-duration impulse usually causes less damage than a more moderate PGA associated with a long duration impulse. In the first case, most of the seismic energy is absorbed by the inertia of the structure with little deformation, whereas in the second case, the more moderate acceleration can result in a significant deformation of the structure due to cyclic loading.

Because structure damage is measured by its inelastic deformation, the earthquake-damage potential depends on the time duration of motion, the energy absorption capacity of the structure, the number of strain cycles, and the energy content of the earthquake. Electric Power Research institute (EPRI, 1988) found that the best correlation between the onset of damage and ground motion occurred when the cumulative absolute velocity (CAV) and the Arias intensity (I_{Arias}) are used. CAV and I_{Arias} are defined by eqn (1) and eqn (2), respectively:

$$CAV = \int_0^t |a(t)| dt \quad (1)$$

$$I_{Arias} = \pi/2g * \int_0^t a(t)^2 dt \quad (2)$$

where t is the total duration of the record, $a(t)$ is the acceleration time history and g is the acceleration of gravity. In both equations, one observes that the time t is reciprocal to the acceleration $a(t)$ for a constant value of CAV and I_{Arias} , respectively.

The current seismic-design practice for structures has different shortcomings: The design is mainly based on strength principles by using the acceleration spectra, and does not directly account for the influence of the duration of the strong motion or for the hysteretic behaviour of the structure. The aim of this paper is to present a hysteresis model for concrete to overcome these shortcomings.

2.2 Behaviour of concrete

When a concrete specimen is monotonically loaded, micro cracks are formed for loads above about 30% of the compression strength. The stable crack growth leads to a disaggregation of the structure of the concrete for loads above about 65% of the compression strength. A critical stress is reached between 75% and 85% of the compression strength when axial cracks are formed, the lateral strain rapidly increases and the volume grows. This critical load describes approximately the fatigue strength (Hohberg, 2004).

Cyclic mechanical loads above the fatigue strength tire the concrete over time. Three phases of permanent deformation, i.e. the damage degree, can be recognized, if one looks at the progress of deformation as function of the number of load cycles. The first phase indicates a large deformation release when crack growth is initiated, the rate of deformation will then lower due to stress rearrangement. The second phase is characterized by a constant, low rate of deformation increase where the damage constantly but little rises due to the formation of micro cracks. The instable crack growth results in the third phase in an excessive increase of the deformation and ultimately to the collapse of the concrete.

It is observed during cyclic loading that the slope of the hysteresis loops is reduced with increasing deformation and that the secants through the hysteresis loops may cut in a common point, the so called pivot point (Hohberg, 2004). One can conclude from the existence of such a pivot point that the cyclic fatigue effects – decrease of stiffness and increase of permanent deformation – are in a linear relation.

3 MATERIAL LAW FOR REINFORCED CONCRETE

3.1 Hysteresis model for concrete

It is assumed that the damaging effect of an earthquake on reinforced concrete buildings can be explained by the cyclic fatigue of concrete. Therefore, the material behaviour of concrete is extended by a hysteresis model. Based on the findings in the literature, the hysteresis model for concrete consists of the following elements (Fig. 1):

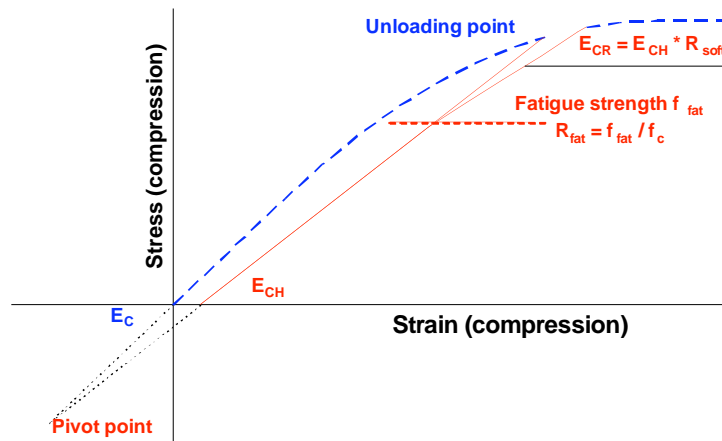


Figure 1. Hysteresis model for concrete.

- The stiffness E_{CH} is newly evaluated at each unloading from the unloading point and the pivot point.
- When the load exceeds the fatigue strength f_{fat} during re-loading, the stiffness E_{CH} is reduced with the factor R_{soft} to the re-load stiffness E_{CR} .
- In the post failure region, the ratio R_{fat} of the current fatigue strength f_{fat}^* to the current strength f_c^* is constant and equal to the ratio of the fatigue strength f_{fat} to the compression strength f_c .

3.2 Material parameters for reinforced concrete

The material law for concrete is defined as it is the rule by a standard, in this case by the Swiss standard SIA 262 (2003), and is extended to describe also the post failure behaviour (Fig. 2). The material parameters for the used concrete C20/25 are according to SIA 262 (2003): Tensile strength $f_{ct} = 2.2 \text{ N/mm}^2$, compression strength $f_c = -28 \text{ N/mm}^2$, ultimate compression strain $\varepsilon_{cu} = -0.003$, modulus of elasticity $E_c = 30'365 \text{ N/mm}^2$. The following parameters are assumed for the hysteresis model for concrete: Tensile strength f_{pivot} at the pivot point = 100 N/mm^2 , fatigue strength ratio $R_{fat} = 0.7$, and softening factor $R_{soft} = 0.8$ for the re-load stiffness E_{CR} .

The behaviour of the used reinforcement B500B is described by a bilinear material law with kinematic hardening and the parameters according to the Swiss standard SIA 262 (2003): Yield limit $f_{sk} = 500 \text{ N/mm}^2$, ultimate strength $f_{tk} = 540 \text{ N/mm}^2$, ultimate strain $\varepsilon_{uk} = 0.050$, modulus of elasticity $E_k = 205'000 \text{ N/mm}^2$.

4 MICROMECHANICAL MODEL

4.1 Model assumptions

The effect of the hysteresis model for concrete is shown on a section through a reinforced concrete wall using a micromechanical model, where the structure is subdivided into small elements. It is assumed that these elements are loaded only uniaxial and do not have any impact on the other elements. The calculations are performed for a wall element of a thickness of 300 mm and a unity depth of 1 mm. The overall wall thickness is divided into 1 mm thick concrete elements. The orthogonal reinforcement is placed on both sides of the wall in a distance of 40 mm from the surface. Three cases are studied: Without reinforcement, reinforcement of $336 \text{ mm}^2/\text{m}$ (diameter 8 mm each 150 mm), and reinforcement of $1334 \text{ mm}^2/\text{m}$ (diameter 16 mm each 150 mm).

4.2 Behaviour of concrete under pure compressive loading

The strain controlled stress-strain diagram for concrete (without reinforcement) is shown in Fig. 2. In re-loading, the two curves for complete and partial unloading require a larger deformation to join again the virgin loading due to the softened stiffness. The filleting between the hysteresis loops and the abscissae as well as the virgin loading is a result of the strain increments, which were chosen too large for these calculations. As a result of the implemented pivot point, the unloading stiffness E_{CH} is reduced in this example from its initial value to about one third in the final stage.

The behaviour of the hysteresis model for concrete during cyclic fatigue is examined for a stress driven cyclic loading between the stress levels σ_{upper} and σ_{lower} . The upper stress level σ_{upper} was increased in the different runs from 0.71 to 0.99 times the maximal stress σ_{max} of monotonic loading. The lower stress level σ_{lower} was kept constant at 0.60 times the compression strength f_c since only stresses above the fatigue strength f_{fat} account for fatigue and σ_{lower} is less than the fatigue strength f_{fat} . Fig. 3 shows the number of cycles needed for collapse. Based on the stress levels 75% and 95%, an approximately constant value for the collapse index I_{coll} (eqn (3)) is achieved with a rather high exponent m : the exponent m takes a value of 8 for concrete and a value of 4 for reinforced concrete. The collapse index I_{coll} for reinforced concrete is similar to the characteristic index I_c (eqn (4)) proposed by Park and Ang (1985). The characteristic index I_c is a parameter that has a reasonable representation of the destructiveness of ground motions because it correlates well with structural damage.

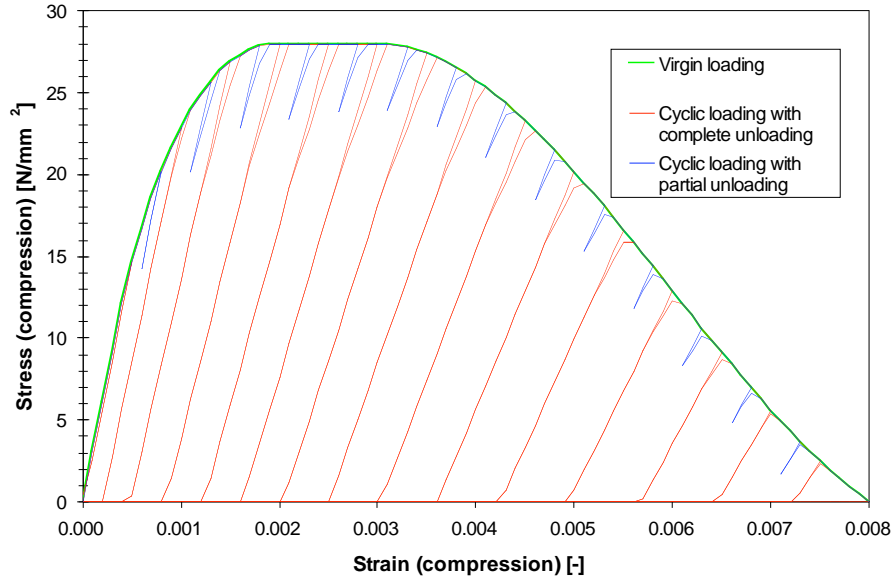


Figure 2. Stress-strain diagram for concrete (without reinforcement) under strain controlled loading.

$$I_{\text{coll}} = \sigma_{\text{upper}}^m * \text{number of load cycles} \quad (3)$$

$$I_c = a_{\text{rms}}^{1.5} * t_s^{0.5} \quad \text{with} \quad a_{\text{rms}}^2 = 1/t * \int_0^t a(t)^2 dt \quad \text{and} \quad t = t_s \quad (4)$$

where σ_{upper} is the upper stress level of the cyclic loading, the exponent m , $a(t)$ is the acceleration time history and t_s is the significant duration of the ground motion. Significant duration t_s is defined as the interval between the times at which 5% and 95% of the Arias intensity I_{Arias} is attained.

Fig. 3 proves that concrete can fail either by a few strong load cycles or by a lot of weak load cycles. However, the large weight of the stress level given by the exponent m indicates that the benefit for higher stress levels may be quite small due to a too small reduction of the number of load cycles.

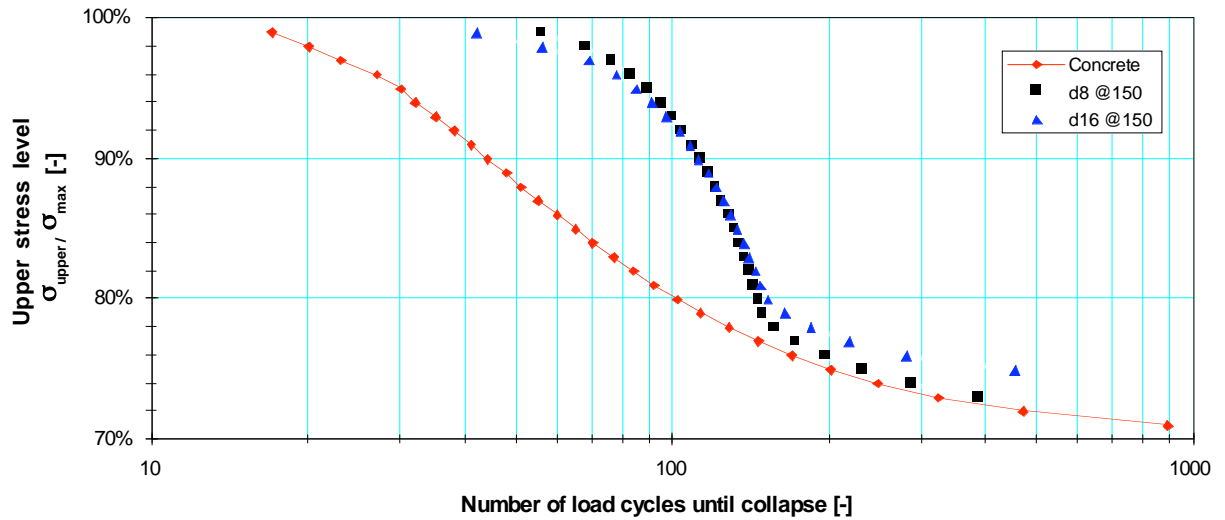


Figure 3. Number of load cycles until collapse.

The first phase with decreasing deformation against the number of load cycles is missed in the fatigue lines of concrete (Fig. 4), since the hysteresis model for concrete neglects the large release of deformation during the initiation of crack growth. The stabilizing effect of a reinforcement helps to form also the first phase: It is well pronounced for a reinforcement with diameter 16 mm each 150 mm which demonstrates the effect of reinforcement to inhibit the structure from collapse as long as concrete is not loaded far beyond the fatigue strength. The second phase with a constant deformation rate is roughly reached: The small increase of the rate of deformation with load cycles is a result of the assumed weakening by the applied pivot point.

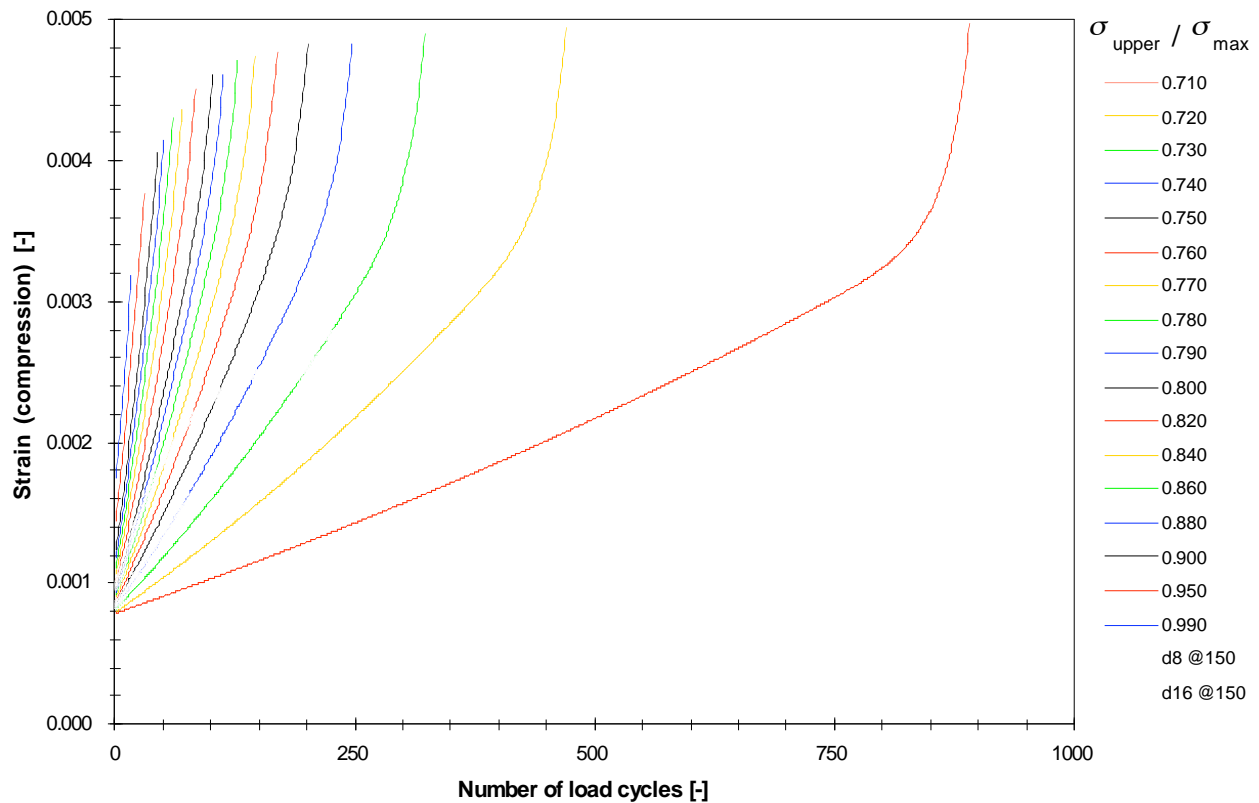


Figure 4. Fatigue lines for different upper stress levels σ_{upper} .

The beginning of the third phase with the excessive increase of deformation leading to collapse is only recognized for lower stress levels σ_{upper} .

4.3 Behaviour of concrete under pure shear loading

Basis for the assessment under shear loading are inclined compression fields with uniaxial compression and constant stress intensity. The compression fields are taken by the concrete, whereas the compensating tensile forces are taken by the reinforcement. Since the pressure field acts like concrete under pure compression loading, shear loading of reinforced concrete will not be looked at separately.

4.4 Behaviour of reinforced concrete under pure bending loading

The form of the load cycles is mainly driven by the reinforcement through its elastic and its plastic material behaviour. During the first cycle, one observes a very stiff loading and unloading (Fig. 5) until the bending moment drops due to the cracked concrete. The further cycles exhibit a bend in the elastic deformation phase of the reinforcement when the compressed concrete is unloaded and the cracks start to open. Beginning with cycle 5, a jump in the bending moment is observed, when the cracks close in the plastic deformation phase of the reinforcement. Collapse is reached in the eighth cycle when concrete starts to crush.

The number of load cycles could not be determined in bending loading when the bending moment is varied between an upper value M_{upper} and a lower value M_{lower} of about half the maximum bending moment M_{max} in monotonically loading. This behaviour is well-founded in that the reinforcement is cyclic loaded in a range with practical constant strain limits. Because of this strain limitation, the concrete can degrade only by reducing the loading in each cycle as long as the fatigue strength is reached well before the concrete collapses.

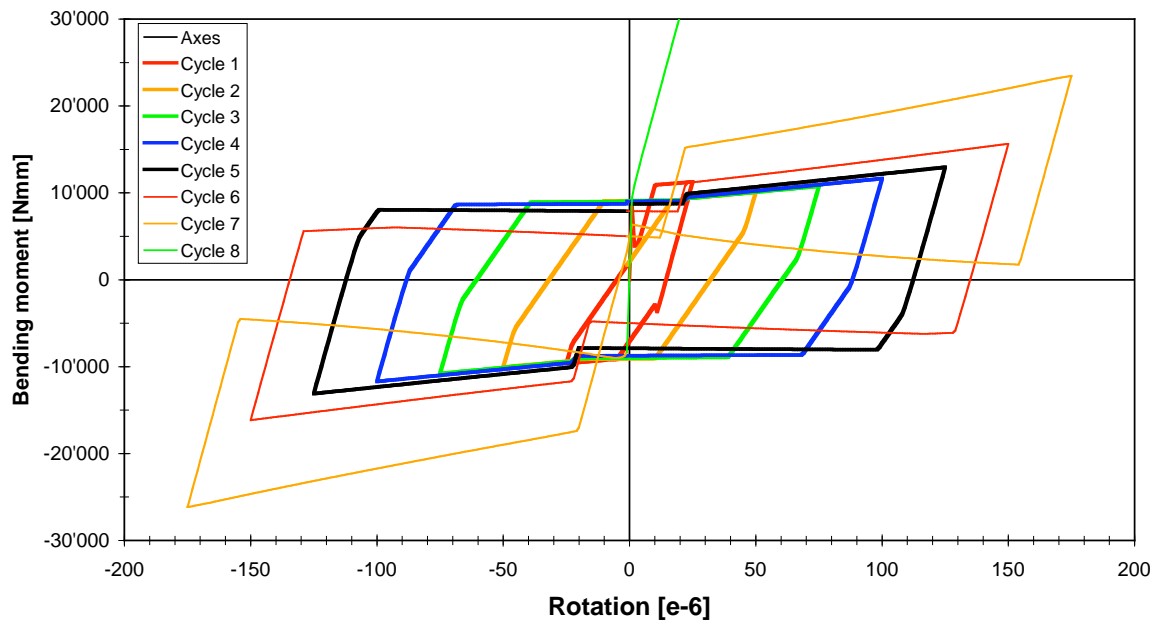


Figure 5. Bending moment-rotation diagram for reinforced concrete (d8 each 150 mm) under rotation controlled loading.

5 FINITE ELEMENT ANALYSES

5.1 Implementation of the hysteresis model for concrete into a finite element code

The hysteresis model for concrete was implemented as a user supplied material model into the finite element code ADINA (1984). The user supplied material model is based on the three dimensional concrete model of ADINA. An equivalent isotropic material law is assumed based on the deviatoric stress-strain relationship. Since this paper is focused on the effect of the hysteresis behaviour, tension cut-off is neglected for the concrete.

5.2 Effects of earthquakes to a reinforced concrete building

A cubical structure with outer dimensions 3.5 m*3.5 m*3.5 m was chosen as an example. The thickness of the concrete walls is 0.25 m, and the orthogonal reinforcement on both sides of the wall is taken to be 1334 mm²/m (diameter 16 mm each 150 mm). The base of the building is completely fixed. The density of the concrete in the roof plate is increased from 2500 kg/m³ to 420'000 kg/m³ to lower the resonance frequency. Thus, the additional mass of 1.28*10⁶ kg brings the resonance frequency down to 9 Hz. In the finite element code, the concrete is simulated by 8-noded three-dimensional solid elements with side length 0.25 m, and the reinforcement by 4 noded two-dimensional solid elements with side length 0.25 m and appropriate thickness.

Basis for the earthquake loading is the design response spectrum according to the Regulatory Guide 1.60 (1973) for a damping of 5%, and anchored to a PGA of 0.375 g. With the same seed, two artificial time histories are generated for magnitude M5.5 and M7.0. The time histories are multiplied by a tripartite function to result in a parabolic rise to unity at a rise time T_r , a plateau of value unity for the strong motion duration T_s , and a linear ramp down to zero for a decay time T_d . These time parameters as functions relating to a specified earthquake magnitude estimate (M) are determined by fitting empirical data obtained from Salmon et al (1992) and are given in Table 1. The time histories are base line corrected to result in zero velocity and zero displacement after the earthquake. During the calculations, a tremendous effect of small changes in the time histories has been observed. Therefore, the time history of magnitude M7.0 has been merged from the time history of magnitude M5.5 till the end of the strong motion (i.e. till 6.065 s) and from the tail (after 6.065 s) of the original time history for magnitude M7.0 (Fig. 6).

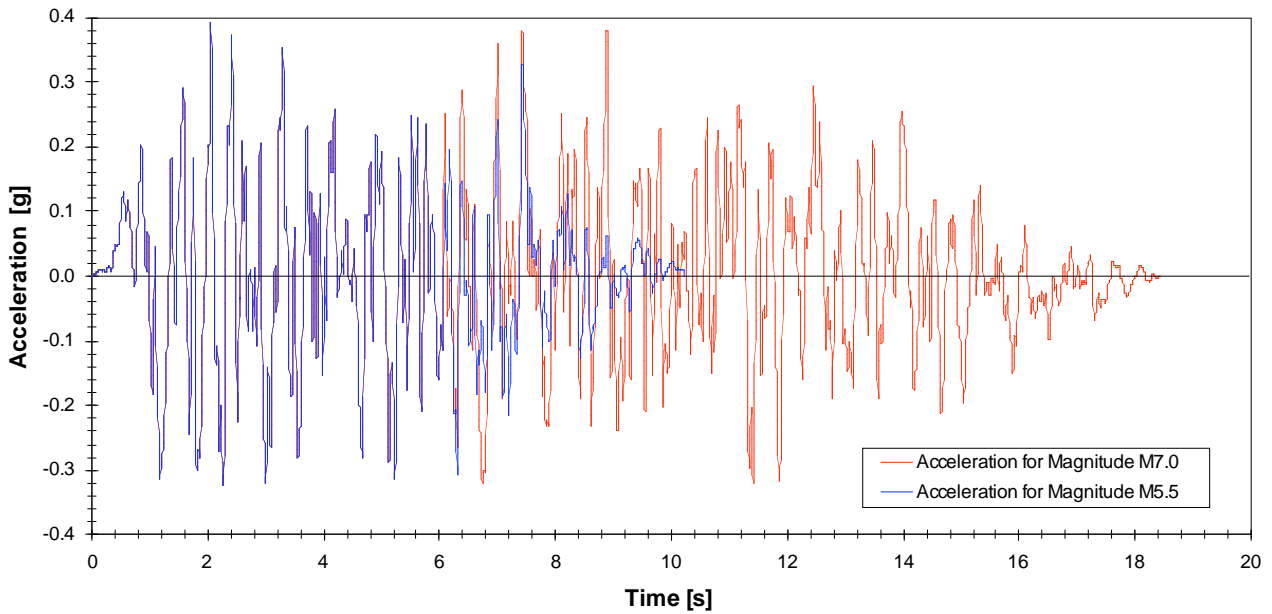


Figure 6. Artificial time histories for Magnitude M5.5 and Magnitude M7.0 used for comparison.

Table 1. Time parameters used for the artificial time histories.

magnitude M	rise time T_r	strong motion duration T_s	decay time T_d	total duration
5.5	1.260 s	4.805 s	4.165 s	10.230 s
7.0	2.240 s	9.735 s	6.705 s	18.680 s

It was found in a parametric study that the same damage state of the building is reached when the acceleration amplitudes are increased in the case of magnitude M5.5 by a factor of 1.25, and when they are kept constant in the case of magnitude M7.0. The evolution of the maximal deviatoric strain is depicted in Fig. 7 for both earthquakes. The maximal value of Fig. 7 indicates that the maximal strength of the concrete is just reached. Since the heavily damaged material is concentrated in same small regions, the hysteresis behaviour is of minor importance for the overall behaviour of the structure.

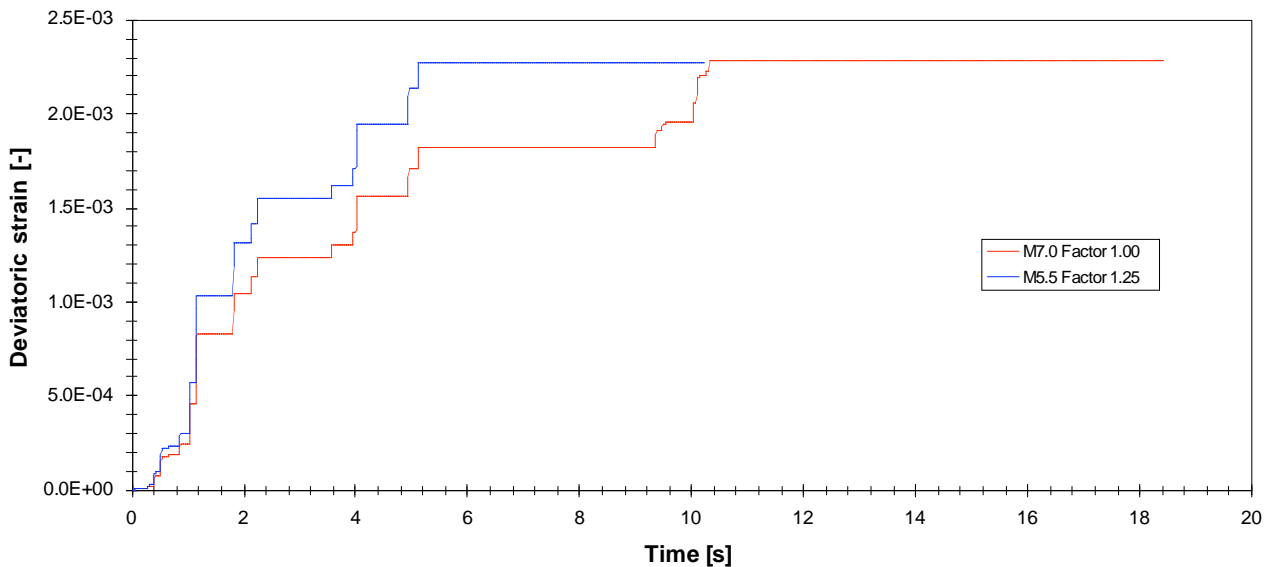


Figure 7. Deviatoric strain as measure for the damage state.

Table 2 shows the CAV value, the Arias intensity I_{Arias} , the acceleration during strong motion a_{rms} , and the characteristic index I_c of Park and Ang for the same damage state, when the strength of the concrete is reached. None of these parameters give identical values for both magnitudes. Hence, this study shows no favoured parameter as a predictor for collapse.

Table 2. Ground motion parameters for the same damage state of the building, when the strength of concrete is reached.

magnitude M	PGA	CAV eqn (1)	I_{Arias} eqn (2)	a_{rms} in eqn (4)	I_c eqn (4)
5.5	0.469 g	1.230 gs	0.409 gs	0.196 g	0.0418
7.0	0.375 g	1.791 gs	0.475 gs	0.148 g	0.0153

6 CONCLUSION

- A hysteresis model for concrete was presented, which accounts for the degradation of concrete.
- It was demonstrated by means of the hysteresis model for concrete in a micromechanical model for a reinforced concrete wall under cyclic loading:
 - Under compression and shear loading, strong earthquakes need less load cycles than weak ones until the concrete collapses.
 - The hysteresis model accounts for the three phases of fatigue with decreasing, constant and excessively increasing rate of deformation with the number of cycles.
 - At pure bending, the reinforcement dominates the behaviour whereas the influence of concrete is marginalized.
- A simplified reinforced concrete building was studied for two earthquakes of magnitude M5.5 and M7.0, respectively:
 - Damage is reached for the earthquake of magnitude M5.5 at a higher PGA than for the earthquake of magnitude M7.0.
 - This study shows no favoured parameter as a predictor for collapse.
 - It is obvious, that the level of the PGA is not a measure for the damage of buildings.

REFERENCES

- EPRI 1988. A criterion for determining exceedance of the operating basis earthquake. EPRI NP-5930. Electrical Power Research Institute, Palo Alto, California.
- Hohberg, R. 2004. Ermüdungsverhalten von Beton. Technische Universität Berlin, Thesis.
- Park, Y. J., Ang, A. H.-S. 1985. Mechanistic seismic damage model for reinforced concrete. J. Struct. Eng., ASCE, 111, no. ST4. P. 722-739.
- Regulatory Guide 1.60 1973. Design Response Spectra for Seismic Design of Nuclear Power Plants. U.S. Nuclear Regulatory Commission, Rev. 1.
- SIA 262 2003. SIA Norm 262 – Betonbau. Schweizerischer Ingenieur- und Architektenverein, Zürich (CH).
- Salmon, M.W., Short S.A. and Kennedy, R.P. (1992). Strong Motion Duration and Earthquake Magnitude Relationships. USDOE, UCRL-CR-117769.
- ADINA 1984. Automatic Dynamic Incremental Nonlinear Analysis – Users manual. ADINA Engineering, Watertown (MA/USA).